

LASERS

PACS numbers: 42.55.Px; 42.60.Da; 42.60.Fc; 42.62.Eh
DOI: 10.1070/QE2009v039n06ABEH013955

Low-threshold short-cavity diode laser for a miniature atomic clock

S.V. Kargapol'tsev, V.L. Velichansky, V.V. Vasil'ev, M.Sh. Kobyakova, A.V. Morozyuk, N.V. Shiryaeva, V.P. Konyaev

***Abstract*. Short-cavity diode lasers (SCDLs) emitting at the 894-nm D_1 line of caesium are developed. Low threshold currents and power consumption will make it possible to use these lasers in chip-size atomic clocks (CSACs) and magnetometers. The SCDL parameters are comparable with the parameters of surface-emitting lasers.**

Keywords: *diode laser, coherent population trapping resonance, chip-size atomic clock.*

1. Introduction

The development of chip-size (~ 1 cm^3) low-power atomic clocks on hyperfine transitions in Rb and Cs attract great recent interest [1 – 3]. Such atomic clocks can be used in portable two-directional broadband radio receivers and transmitters for protecting information being transmitted, for synchronising telecommunication networks, in instrument engineering, in GPS receivers with the increased performance and noise immunity [4, 5] and in similar GLONASS receivers being developed in Russia. The mass production of miniature, cheap and precise clock generators will make it possible to use them in cell telephones.

Compact quartz generators have low power consumption and at the same time a relatively low long-term stability (the relative frequency deviation per 24 hours is $10^{-5} - 10^{-7}$) mainly due to the temperature drift. The best quartz generators with a high long-term stability ($10^{-9} - 10^{-10}$ per 24 hours) have a comparatively large volume (more than 50 cm^3) and high power consumption (~ 3 W) [6]. Transportable atomic frequency standards have a high long-term stability but their dimensions and power consumption are larger than those of quartz generators. In the course of many years' work on reducing the dimensions of optically-pumped atomic clocks, the volume of these devices has achieved 100 cm^3 [7]. In these clocks the probing microwave field directly affects the atoms in the microwave cavity. The further possible decrease in the overall dimensions is limited by the fact that the characteristic dimension of the microwave cavity is comparable with the wavelength of the microwave field [8]. For instance, the wavelength of the transition between hyperfine sublevels of the ground state in Cs is ~ 3.2 cm.

A new approach to the formation of a reference resonance in atomic clocks has been intensely studied in the last years. It is based on the effect of coherent population trapping (CPT) in a bichromatic laser field [9, 10]. As in the case of the traditional approach, which employs the optical-radio-frequency double resonance, the microwave generator frequency is stabilised in new generation miniature atomic clocks. However, the microwave field does not directly interact with the atoms but serves to produce a bichromatic laser field. The frequency difference of components of this field is equal or multiple of the microwave generator frequency. When it is equal to the frequency of the hyperfine splitting of the ground-state sublevels, a dip in absorption is observed [11, 12]. The transmission dependence of the cell with the atoms on the frequency difference of the bichromatic field components (and the microwave generator frequency) produces a reference CPT resonance (Λ resonance) of the atomic clock.

The advantage of this method consists in the removal of the microwave cavity from the scheme and the possible miniaturisation of the clock. A number of US institutes and companies work now on the program of the development of an atomic clock with the volume ~ 1 cm^3, power consumption 30 mW and relative frequency instability 10^{-11} per hour [1]. An optical quantum discriminator with the 9-mm^3 volume was demonstrated for this clock in [2, 3]. The same discriminator can serve as a basis of a compact magnetometer [13]. In paper [14] the clock volume together with all the electronics is about of 10 cm^3.

Only diode lasers (DLs) are capable of providing the required compactness and small power consumption. In this case, the dynamic parameters of the laser should ensure a high efficiency of microwave modulation without excitation of the multi-mode regime. Vertical cavity surface emitting lasers (VCSELs) meet these requirements. Because these lasers are not manufactured in Russia, in this paper we use an alternative variant, i.e. diode lasers of the ordinary geometry (edge emitting) but with a relatively short cavity (SCDLs).

2. Requirements for bichromatic radiation

Spectral characteristics. Two-frequency continuous radiation at the resonance D_1 lines of Rb ($\lambda = 794.8$ nm) and Cs

S.V. Kargapol'tsev, V.L. Velichanskii, V.V. Vasil'ev P.N. Lebedev Physics Institute, Russian Academy of Sciences, Leninsky prosp. 53, 119991 Moscow, Russia; e-mail: sergka@rambler.ru;
M.Sh. Kobyakova, A.V. Morozyuk, N.V. Shiryaeva, V.P. Konyaev M.F. Stel'makh Polyus Research and Development Institute, ul. Vvedenskogo 3, 117342 Moscow; Russia

Received 8 August 2008; revision received 15 October 2008
Kvantovaya Elektronika **39** (6) 487 – 493 (2009)
Translated by I.A. Ulitkin

($\lambda = 894.6$ nm) is required in miniature CPT clocks. The frequency interval between the laser field components should be equal to the hyperfine splitting Δ_{hf} of the alkali metal ground state, which is $\sim$3.030, 6.835 and 9.193 GHz for ^{85}Rb, ^{87}Rb and ^{133}Cs, respectively. At the modulation with the frequency f, either two first side bands ($f = \Delta_{hf}/2$) or one of them and a carrier band ($f = \Delta_{hf}$) are used. It is important that there are no strict requirements to the spectral width of each of the resonance field components. In the majority of probing methods, the admissible width is 1 GHz and in the scheme proposed in [15] the width should be smaller that the splitting of the $5P_{1/2}$ level in ^{87}Rb (812 MHz), i.e. no more than 100 MHz. However, the mutual coherence of two components should be high, i.e. their frequency fluctuations should be correlated [12, 16]. The measure of the mutual coherence is the spectrum width of beatings of these components, which should be an order of magnitude smaller than the width of the CPT resonance. For the 1 – 10-kHz widths of the reference microwave resonance realised in the cells of the volume of a few cubic millimetres, the spectral width of beatings should not exceed 0.1 – 1 kHz.

Polarisation. The optimal variant is when the polarisation of both components is linear and orthogonal to each other [17]; however this variant is not very simple to realise technologically. Another possible variant is when both components have the identical circular polarisation although it leads to a noticeable decrease in the resonance contrast because of the additional 'trapping' states. Both these variants are suitable for ^{85}Rb, ^{87}Rb and ^{133}Cs atoms. The simplest variant for two identical linear polarisations (with a high contrast of the reference resonance) is possible only for the ^{87}Rb isotope and not at high pressures of the buffer gas [15].

Power and threshold current. In papers [2, 3] the total output power at the cell input was 12 and 3.5 μW at beam diameters of 0.25 and 0.125 mm, respectively. At the beam diameters 1 – 2 mm, the output power can achieve 100 μW without increasing the field broadening of the reference resonance. There are two reasons according to which the DL output power should exceed the output power at the cell input. Near the threshold, both frequency and amplitude output noises are maximal so that it is desirable to have a significant excess of the pump current over its threshold. In addition, the DL operation is sensitive to parasitic optical feedback, which can be suppressed by neutral filters. When the filter with the transmission 0.1 – 0.03 is used, reflected radiation will be attenuated by 10^{-2} – 10^{-3} times. Most of the above DL applications assume low power consumption, which means that the threshold current should not exceed several milliamperes.

3. Methods for producing a bichromatic field

There exist a number of methods for two-frequency field generation, which employ: (i) two independent mode-locked DLs [18]; (ii) radiation phase locking to the harmonics of the frequency comb generator [19]; (iii) one laser, which stably generates one frequency at the resonance line, and the second laser (with the microwave modulation of the pump current), whose frequency is captured by the output frequency of the first laser [14]; (iv) electro-optical modulation of laser radiation [20]; (v) different longitudinal modes of one laser [21]; (vi) two independent diode lasers with the microwave modulation of the current, which has the corresponding relative phase delay [22]; (vii) two independent highly-coherent external cavity lasers [23]; (viii) microwave modulation of the DL current [9].

The advantage of the first two and the sixth methods is the possibility of the independent control of polarisation and amplitudes of the field components, stability of the regime and absence of redundant spectral components. The main advantage of the last method is its simplicity. The disadvantages of all the methods, except for the last one, is the complexity and large dimensions of devices fabricated on their bases. If the modulation frequency is equal to half the frequency of the hyperfine splitting of the ground state, only the first two side bands are the working. However, apart from them, the carrier and higher-frequency bands are present in the general case. These 'redundant' components decrease the signal/noise ratio and change the resonance frequency of the microwave transition due to the light shift (dynamic Stark effect). In addition, during this modulation side bands have equal polarisations and one of the methods for obtaining the high contrast of the Λ resonance is bichromatic radiation in which linear polarisations of the components are orthogonal [17]. Nevertheless the method of high-frequency modulation of the laser current is the most acceptable for miniature atomic clock. To realise it requires only one radiation source and no additional optical elements. It is this method that was used in [2, 3, 13].

4. Requirements for lasers

VCSELs are the most suitable radiation source for the problem under study. The cavity lengths of these lasers are so small (several microns) that they always operate at one longitudinal mode. These lasers can have threshold currents less than 1 mA and the working currents of about 2 mA and provide the output power of $\sim$ 1 mW. The power consumption of these lasers does not exceed 5 mW (by neglecting the power spent for thermal stabilisation) and they allow the required high-frequency modulation. Till recently only 852-nm and 780-nm lasers were available, and hence, the first results on the spectroscopy of the CPT resonance were obtained on D_2 lines in Cs and Rb. As was shown in [24] the use of the D_1 line instead of the D_2 line increases the contrast and the ratio of the amplitude of the Λ resonance to its width as well as improves the clock stability. Symmetricom Inc. has recently developed a VCSEL emitting at 894 nm [1] and an optical quantum discriminator of miniature atomic clock employing a 794-nm VCSEL has been demonstrated in [3]. Unfortunately these lasers emitting at the D_1 lines in Cs and Rd are unavailable in Russia. In this paper we propose another approach to the formation of a two-frequency source.

For typical DLs fabricated at the Polyus Research and Development Institute, the threshold current is 25 – 55 mA, the output power is 10 – 50 mW and the cavity length is 600 – 1000 μm. 895-nm lasers are also available. A miniature clock does not require a high output power, moreover, the energy budget of the device restricts it at the level $\sim$ 1 mW. The idea consists in the development of an edge-emitting DL (perpendicular to the current direction) but with a shorter cavity and a high reflection coefficients of mirrors. This will allow one to decrease considerably the threshold current and the laser power consumption and at the same time to increase the stability of the single-frequency regime.

Two variants for fabricating such lasers are possible:

(i) Decrease in the cavity length and threshold current without varying the wavelength. The radiation wavelength of a DL from each new series is usually measured near the lasing threshold at specified values of the cavity length L_0 and reflection coefficients R_1, $R_2 = R_0$ of mirrors (usually, $L_0 = 0.4$ mm and $R_0 = 0.32$). If the initial wavelength is close to the required one (~ 895 nm for the D_1 line in Cs), the problem is reduced to shortening the cavity to the length L and to increasing the mirror reflection coefficients R_1, R_2 to such values at which the generation wavelength remains constant. It is determined (with the accuracy to the order of the intermode interval) by the spectral maximum of the gain. Proximity to the threshold and small variations in the total intensity of counterpropagating waves over the cavity length both for the initial and (moreover) for the short cavity with an increased reflection coefficient of mirrors allow one to neglect the gain saturation and consider the gain g to be constant along the length:

$$g = \alpha - \frac{1}{2L}\ln(R_1 R_2), \tag{1}$$

where α are distributed losses in the cavity and the local gain g is averaged only over the transverse coordinates. In this approximation, both the position of the spectral maximum and the threshold density of the pump current are determined by g. The local gains near the threshold in the initial and shorter cavities are equal, if $R_1 R_2 = R_0^{2L/L_0}$. It is assumed in this case that the distributed losses in the cavity do not change by varying its length. This is quite justified because together with the local gain, the threshold current density and the wavelength of the gain line centre remain constant. The threshold current decreases in this case by L/L_0 times. For example, when the cavity length decreases down to 100 (50) μm, the threshold current decreases by four (eight) times. If the reflection coefficient of one of the short-cavity mirrors is $R_2 \approx 0.98$, the reflection coefficient of the second mirror is $R_1 = 0.58$ (0.77). The output power at the same working current density will decrease but the requirements to the power are very low.

(ii) Change in the threshold current with simultaneous wavelength tuning. If the wavelength in initial samples differs from the required one, apart from the decrease in the generation threshold, it is also necessary to select the cavity parameters and the local gain (the current density) so that the gain line centre of the shortened cavity near the threshold should coincide with the required wavelength. It is desirable that the initial wavelength be shorter than the required one. In this case, it is necessary to decrease the local gain and the threshold current will decrease because of the decrease not only in the cavity length and the contact area but also in its density. In quantum-layer lasers, it is not always possible to predict accurately the dependence of the radiation wavelength on the loss level; that is why in this paper we determined experimentally this parameter.

5. Modulation efficiency

The modulation efficiency of the laser frequency can be realised when the modulation frequency is lower or of the order of the relaxation oscillation frequency of the laser dynamic variables. Therefore, the modulation variant with $f = \Delta_{hf}/2$ is preferable. For small amplitudes, the relaxation oscillation frequency is

$$f_{rel} = \frac{1}{2\pi}\left[\frac{1}{\tau_e \tau_{ph}}\left(\frac{J}{J_{th}} - 1\right)\right]^{1/2}, \tag{2}$$

where J and J_{th} are the densities of the working and threshold pump currents, respectively; τ_e is the lifetime of electrons; τ_{ph} is the lifetime of photons in the cavity. In the case $f = \Delta_{hf}/2$, it is required that the output power should be contained mainly in the first-order side bands. For this purpose, the frequency modulation index m_{fm} should be rather large (for example, $m_{fm} \approx 2$, when the power of the carrier becomes equal to the power of highest side bands). It is expedient to use here the expression, which is valid for a deeper modulation:

$$f_{rel} = \frac{1}{2\pi}\left(\frac{Ap_0}{\tau_{ph}}\right)^{1/2}, \tag{3}$$

where p_0 is the stationary density of photons; A is the constant of the differential optical gain;

$$\tau_{ph} = \frac{1}{\upsilon_{gr}}\left(\alpha + \frac{1}{L}\ln\frac{1}{R}\right)^{-1} = \frac{1}{\upsilon_{gr}}\left[\alpha + \frac{1}{L}\ln(R_1 R_2)^{-1/2}\right]^{-1} = \frac{1}{\upsilon_{gr}} g^{-1}; \tag{4}$$

υ_{gr} is the group velocity of light.

A decrease in the cavity length with a simultaneous increase in the reflection coefficients of the mirrors while preserving invariable the threshold current densities and the local gain g, does not change the lifetime of photons in the cavity.

It is appropriate to compare the relaxation oscillation frequencies of a long-cavity laser and a SCDL at the identical excess over the threshold. In the first variant of the decrease in the cavity length, when g is preserved, photon lifetime in the cavity (4) remains invariable. At the constant electron lifetime τ_e in the stationary regime near the generation threshold, the electron concentration n is related to the direct current density J by the relation:

$$n = J\tau_e/ed, \tag{5}$$

where d is the active region thickness.

Thus, τ_{ph} и τ_e are determined by the quantity of the current excess over the threshold and (2) yields the same result for both cavities. Nevertheless, the passage to the short cavity makes it possible to increase f_{rel}, if the maximal excess is determined by the radiation resistance of the output facet and not by the laser overheating. Note also that shortening of the cavity leads to a decrease in the capacity of the p–n transition, which is important for the efficient high-frequency modulation.

When short cavities are used, the distance between longitudinal modes increases, which facilitates the preservation of one type of oscillations at high modulation frequencies.

6. Comparison of SCDL and VCSEL parameters

The main advantages of VCSELs are: the absence of other longitudinal modes except for the working mode, and, as a

result, the increase in the single-mode regime stability to the high-frequency modulation of the current; the absence of discontinuities in the tuning characteristic; the symmetric radiation field; low power consumption; planar technology. When VCSELs are used in miniature quantum discriminators, a small divergence of their radiation is a disadvantage because at small dimensions of the quantum discriminator it leads to a small diameter of the collimated beam, which, at the same power level, results in the increase in the reference resonance width due to the field broadening.

In some types of VCSELs, uncontrolled polarisation switching and excitation of transverse modes are observed. The SCDL radiation has a larger divergence but unsymmetrical radiation field distribution. Because of the discontinuities in the tuning characteristics, the yield of samples suitable for manufacturing SCDLs is $\sim 30\,\%$. On the other hand, the presence of the longitudinal mode comb facilitates tuning the laser line to the atomic line. Both types of the lasers require the gain line centre to be close to the atomic line. The tuning of the only longitudinal VCSEL mode to the atomic line can require a significant change in the laser temperature.

7. Experimental results

In the experiment we used the triple InGaAs solid solution. Experiments were performed using laser diodes with a 3-μm-wide mesastripe (p-contact). The active element was made from a wafer grown by using the MOVPE method. The layer compositions and thicknesses are presented in Table 1.

Table 1.

Layer	Layer composition	x	Layer thickness/μm
Contact	p^+-GaAs	–	0.29
P emitter	$Al_xGa_{1-x}As$	0.337	1.71
P waveguide	$Al_xGa_{1-x}As$	0.291	0.2
Active	$In_xGa_{1-x}As$		0.02
N waveguide	$Al_xGa_{1-x}As$	0.291	0.2
N emitter	$Al_xGa_{1-x}As$	0.337	3
Buffer	n^+-GaAs	–	0.49
Substrate	GaAs	–	80

The electroluminescence wavelength of the active $In_xGa_{1-x}As$ layer was 889 nm. The active elements were mounted with their n-contact on the surface of the copper contact plate with the help of indium. The dependence of the laser wavelength λ_g on the distributed loss level in the cavity for this plate is shown in Table 2 and Fig. 1. To vary losses we manufactured lasers with different cavity lengths and different reflection coefficients of the front (R_1) and rear (R_2) faces. The monotonic dependence of the laser wavelength on losses (Fig. 1) allowed one to determine the optimal reflection coefficients of mirrors for the laser with $L = 100$ μm (light point in Fig. 1) and to produce a batch of such lasers. They oscillated at the wavelength close to the D_1 line in caesium and their threshold currents were from 3.7 to 3.9 mA at temperature 21 °C. At the current 5 mA, the output power was ~ 1 mW.

The laser parameters were studied on the setup, which is presented schematically in Fig. 2. The laser current was

Table 2.

R_1	R_2	L/μm	λ_g/nm	$-(2L)^{-1} \times \ln(R_1R_2)$/cm^{-1}
0.32	0.32	200	870	57
0.32	0.32	400	893	28.5
0.32	0.32	600	897	19
0.32	0.32	100	847	114
0.32	0.98	100	870	58
0.65	0.98	100	895	22.5
0.85	0.98	100	902	9

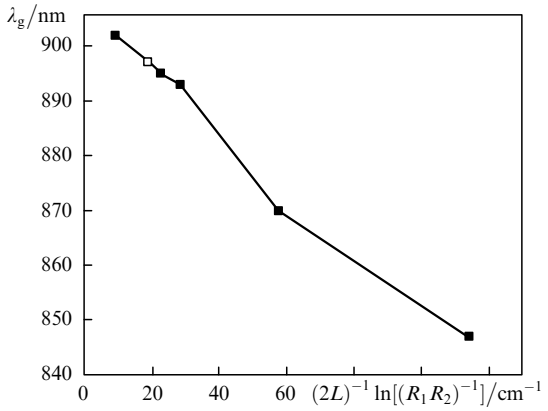

Figure 1. Dependence of the laser wavelength on mirror losses distributed along the cavity length for diode lasers with different mirror reflection coefficients R_1, R_2 and the cavity length L.

modulated by the microwave signal from the Agilient E8257C generator via a T-connector (RF&DC ZFBT-6GW-FT). The SCDL was placed in a closed housing with a holder, which had a double thermal stabilisation contour. Radiation via a system of mirrors and beamsplitters was directed to the cell C1 placed in a solenoid and a magnetic screen, to the additional cell C2, to the fibre of the wavelength meter (LM-600 λ-meter, the measurement accuracy is 0.01 nm) and to the Fabry–Perot interferometer. Radiation was detected using photocells PD1–PD3. Below we present the experimental dependences obtained for one laser but typical for the whole batch.

Each laser is characterised by temperature and current regions in which lasing occurs at a single mode. Figure 3 shows the ranges of temperature wavelength tuning of the mode in the region of the D_1 line in Cs (at the constant current $I = 6.5$ mA) and the current tuning (at the constant temperature $T = 21.5$ °C). At the edges of the tuning ranges lasing switches to another mode, which is approximately 1 nm away. It is interesting that in the case of temperature tuning at the constant current the tuning region (0.34 nm) is approximately twice larger than in the case of current tuning (0.16 nm). During the laser tuning in large frequency ranges, temperature and current tuning intervals coincide on average. When the laser temperature and current are consistently changed, the laser wavelength can be preserved constant. This makes it possible to change the output power without its frequency detuning from the resonance line. Figure 4 presents the dependences of the laser temperature and its output power on the pump current at the constant laser wavelength tuned to the frequency of the hyperfine transition $6S_{1/2}$, $F = 3 \rightarrow 6P_{1/2}$, $F' = 4$ of Cs atoms. In fact, the figure presents the temperature of the sensor fastened on the

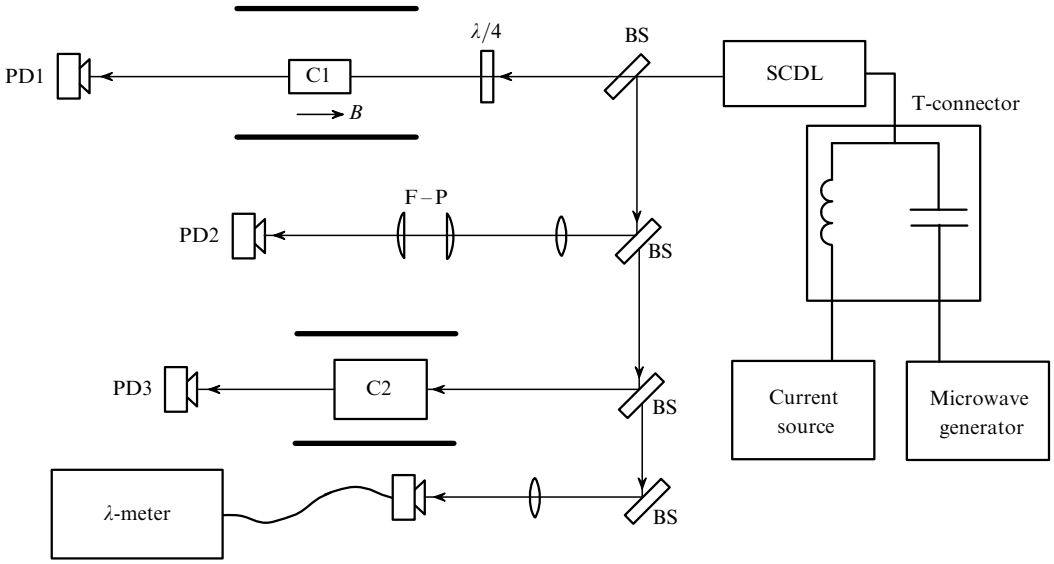

Figure 2. Scheme of the setup: (SCDL) short cavity diode laser; (PD1 – PD3) photocells; (C1) cell with vapours of CS and buffer gas Ar (95 Torr); (C2) additional cell with Cs vapours; (F – P) confocal Fabry – Perot interferometer with a free spectral range of 7.5 GHz; (BS) beamsplitters.

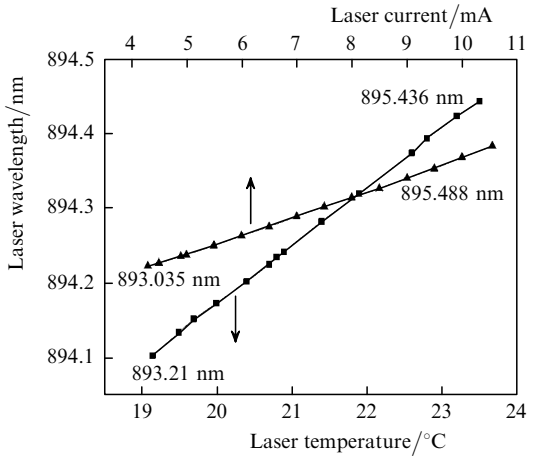

Figure 3. Dependences of the laser wavelength on the current (at the constant temperature 21.5 °C) (▲) and on the laser holder temperature (at a direct current of 6.5 mA) (■). The wavelengths of the modes to which lasing switches are shown at the boundaries of the cw tuning region.

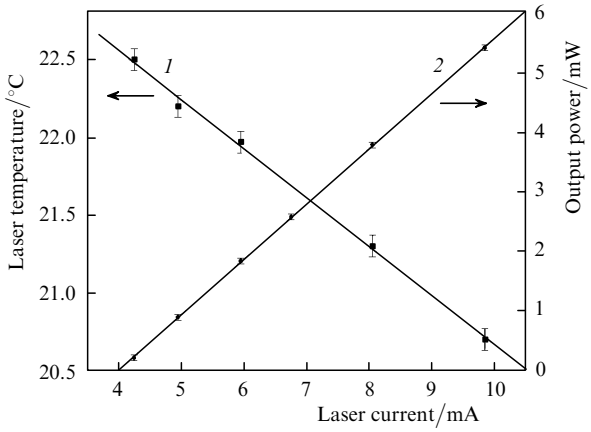

Figure 4. Dependences of temperature (*1*) and power (*2*) on the pump current at a fixed laser wavelength corresponding to the $F = 3 \rightarrow F' = 4$ transition of the D_1 line in Cs.

laser holder at a distance of a few millimetres from it (it is somewhat lower than the temperature of the active region).

To study the frequency dependence of the modulation efficiency of side bands, the laser current was modulated at the frequencies from 0.5 to 5 GHz. We estimated the ratio of the carrier and side band powers with the help of an interferometer with a free dispersion region of 7.5 GHz. This interferometer makes it possible to evaluate the range of the continuous frequency tuning and the degree of adjacent mode suppression. The modulation parameters of the laser are shown in Fig. 5. Frequency-dependent parameters of the laser and the microwave channel contribute to modulation parameters. Figure 5 shows the dependences of the output power in the first order side band on the microwave modulation frequency of the laser at the constant input modulation power of ~ 0.03 mW. The peaks (local maxima) on the curves are determined by the frequency of relaxation oscillations. One can see that the

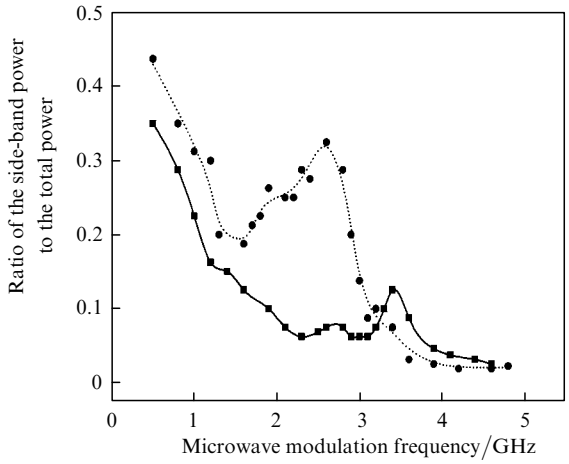

Figure 5. Dependences of the ratio of the power in the first-order side band to the total power of laser radiation on the microwave modulation frequency at the 30-μW output power of the microwave generator and the laser current 7 (●) and 9 (■) mA.

maximum is shifted to larger frequencies at a larger current. Small-scale variations in the dependences are caused by the change in the reflection of the microwave field from the laser crystal and from the sites of microwave radiation coupling upon variation in the frequency of the microwave modulation.

To tune to the centre of the interval between two components of the absorption lines from different hyperfine sublevels of the ground state with $F = 3$ and $F = 4$, apart from microwave modulation of the laser current at the frequency 4.596315885 GHz, we used a saw-like modulation at the frequency 25 Hz. The power of the microwave modulation (4 mW) ensured redistribution of up to 25 % of the total output power to each side band. For tuning, we used the absorption spectrum at the D_1 line of Cs in the additional optical cell (of length 5.5 cm and of diameter 4 cm). Figure 6 presents the change in the output power propagated through the cell upon current scanning of the emission spectrum consisting of the carrier, two dominating side bands and highest-order bands. The slope of the curve is explained by the change in the laser power during the current tuning (low-frequency current modulation). Each component of the spectrum has four Doppler contours for the $F = 3, 4 \rightarrow F' = 3, 4$ transitions. The central resonances A and B correspond to the coincidence of the first two side bands with the components of the resonance doublet (A corresponds to $F' = 4$, B – $F' = 3$). The pairs of adjacent resonances on the left and on the right from the central resonances correspond to the coincidence of the carrier (and highest-order side bands) with the resonance doublet, etc.

By using this laser we observed CPT resonance in caesium. The laser was tuned to the top of the Doppler contour A or B. Figure 7 presents the central CPT resonance corresponding to the metrological 0–0 transition observed in the screened cell of length 3 cm and diameter 2.5 cm, which contained saturated Cs and Ar vapour (95 Torr) in the longitudinal magnetic field. The contrast of the CPT resonance with respect to the background absorption was 4 % at the temperature 30 °C. The resonance is not optimised with respect to the laser field intensity and the cell temperature. The resonance width ($\sim$ 1.1 kHz) coincides with the width obtained earlier in the same cell and at the same intensities of laser radiation by using the polychromatic coherent laser radiation, whose central frequency is locked to the frequency of the external-cavity master laser [25]. The inset shows all seven CPT resonances corresponding to the Zeeman splitting of the $6S_{1/2}$ sublevel (we used a cell without a buffer gas but with an AR coating).

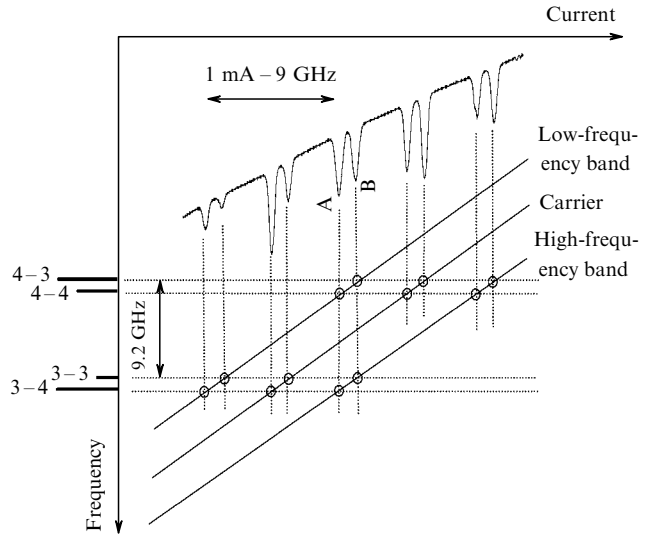

Figure 6. Dependence of the transmission of a three-frequency laser field by the cell with Cs vapours on the laser pump current upon tuning in the region of the D_1 line (top). At the bottom, solid slanting line shows the change in the wavelengths of carrier and side bands. Horizontal dashed lines correspond to four components of the D_1 line. Their relative intensities are shown on the left. Observation conditions of the CPT resonance are fulfilled only for two central peaks A and B.

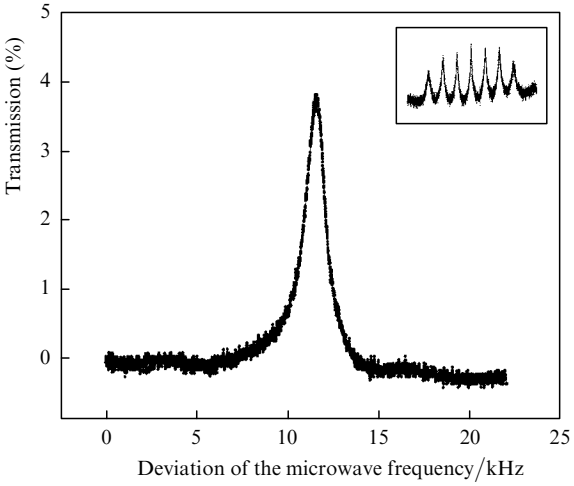

Figure 7. CPT resonance corresponding to the 0–0 transition in Cs obtained in a cell filled with argon (95 Torr) at the intensity of incident radiation 2.9 mW cm^{-2}. The resonance FWHM is 1.1 kHz, the contrast with respect to the background absorption is 4 %. Other resonances are detuned by the longitudinal magnetic field. The inset shows seven CPT resonances (the number of the Zeeman components of the hyperfine $F = 3$ sublevel of the ground state in caesium) recorded in a cell with an AR coating in the magnetic field $\sim$ 3 μT. The interval between adjacent resonances is 12 kHz.

8. Conclusions

A variant of diode lasers for a small atomic CPT clock has been proposed, which can be used instead of vertical cavity surface emitting lasers. A batch of seventeen 100-μm-long samples with the threshold current less than 4 mA and the laser wavelength $\sim$ 894 nm has been manufactured. Four samples at the working current of 5 mA operated in the continuous single-frequency regime with the output power of 1 mW. When changing the current modulation frequency near 4.6 GHz, we observed the CPT resonance produced by two first side bands in the cell with the vapours of Cs and buffer gas. At present, life tests of SCDLs are being performed. This paper is especially important from the point of view of fabrication of domestic devices, because Russia lacks for the technology on the production of vertical cavity lasers. SCDLs can find applications in transportable magnetometers widely used in geological prospecting. Note that in June 2007 Honeywell Co. announced the fabrication a miniature atomic clock (including all electronic components except for the battery with the relative instability of the reference frequency 5×10^{-12}, volume 1.7 cm^3 and power consumption 57 mW [26].

References

1. Lutwak R., Emmons D., English T., et al. *Proc. 35th Annual Precise Time and Time Interval (PTTI) Systems and Application Meeting* (San Diego, CA, 2003) pp 1510 – 1530.
2. Knappe S., Shah V., Schwindt P., Hollberg L., Kitching J., Liew L., Moreland J. *Appl. Phys. Lett.*, **85**, 1460 (2004).
3. Knappe S., Schwindt P., Shah V., Hollberg L., Kitching J. *Opt. Express*, **13**, 1249 (2005).
4. Vig J. *IEEE Trans. Ultrason. Ferroellectr. Freq. Control.*, **40**, 522 (1993).
5. Kuster J.A., Adams C.A. *RF Design*, May 1999, pp 28 – 38.
6. www.marion.ru
7. Gerginov V., Knappe S., Schwindt P.D.D., Shah V., Liew L., Moreland J., Robinson H.G., Hollberg L., Kitching J. *Techn. Dig. Joint IEEE Intern. Freq. Cont. Symp. and Precise Time and Time Interval (PTTI) Syst. and Appl. Meet.* (Vancouver, Canada, 2005) p. 758.
8. Vanier J., Levine M., Janssen D., Delaney M. *Proc. 6th Symp. Frequency Standards and Metrology* (Fife, Scotland: University of St Andrews, 2001) p. 155.
9. Cyr N., Tetu M., Breton M. *IEEE Trans. Instr. Measur.,* **42**, 640 (1993).
10. Vanier J. *Appl. Phys. B*, **81**, 421 (2005).
11. Arimondo E. *Progress in Optics*. Ed. by E. Wolf (Amsterdam, Elsevier, 1996) Vol. XXXV, p. 251.
12. Agap'ev B.D., Gornyi M.B., Matisov B.G., Rozhdestvenskii Yu.V. *Usp. Fiz. Nauk*, **163**, 1 (1993).
13. Schwindt P., Knappe S., Shah V., Hollberg L., Kitching J. *Appl. Phys. Lett.*, **85**, 6409 (2004).
14. Lutwak R., Deng J., Riley W., Varghese M., Leblanc J., Teplot G., Mescher M., Serkland D.K., Geib K.M., Peake G.M. *Proc. 36th Annual Precise Time and Time Interval (PTTI) Syst. and Appl. Meet.* (Washington, DC, 2007) p. 339.
15. Zibrov S.A., Velichansky V.L., Zibrov A.S., Taichenachev A.V., Yudin V.I. *Pis'ma Zh. Eksp. Teor. Fiz.*, **82**, 534 (2005).
16. Fleischhauer M., Imamoglu A., Maraugos J. *Rev. Modern Phys.*, **77**, 633 (2005).
17. Jau Y.Y., Miron E., Post A.B., Kuzma N.N., Happer W. *Phys. Rev. Lett.*, **93**, 160802 (2004)
18. Brant S., Nagel A., Wynands R., Meschede D. *Phys. Rev. A*, **56**, (1997).
19. Akimov A.V., Kolachevskii N.N., Sokolov A.V., Matveev A.N., Kanorskii S.I., Kits R.A., Papchenko A.A., Sorokin V.N. *Kvantovaya Elektron.*, **34**, 983 (2004) [*Quantum Electron.*, **34**, 983 (2004)].
20. Mustel' E.R., Parygin V.N. *Metody modulyatsii i skanirovaniya sveta* (Light Modulation and Scanning Methods) (Moscow: Nauka, 1970).
21. Fadyushin A.B., Velichansky V.L., Lukin M.D., Senkov N.V., Scully M.O., Fleischauer M. *Kvantovaya Elektron.*, **32**, 597 (2002) [*Quantum Electron.*, **32**, 597 (2002)].
22. Shah V., Knappe S., Schwindt P.D.D., Gerginov V., Kitching J. *Opt. Lett.*, **31**, 2335 (2006).
23. Akulshin A.M., Celikov A.A., Velichansky V.L. *Opt. Commun.*, **84**, 139 (1991).
24. Stahler M., Wynands R., Knappe S., et al. *Opt. Lett.*, **27**, 1472 (2002).
25. Bouyer J., Breant C., Schanne P. *Proc. SPIE Int. Soc. Opt. Eng.*, **1837**, 324 (1992).
26. Younger D.W., Lust L.M., Carlson D.R., et al. *The 14th Intern. Conf. on Sol.-State Sensors, Actuators and Microsystems* (Lyon, France, 2007) p. 39.